Am J Physiol Gastrointest Liver Physiol
281: G1487–G1493, 2001.

Regulation of human jejunal transmucosal resistance and MLC phosphorylation by Na^+-glucose cotransport

JESSICA J. BERGLUND,[1] MARTIN RIEGLER,[2] YEVGENY ZOLOTAREVSKY,[1]
ETIENNE WENZL,[2] AND JERROLD R. TURNER[1]
[1]*Department of Pathology, Wayne State University, Detroit, Michigan 48201;*
and [2]*University Clinic of Surgery, Vienna General Hospital, A-1090 Vienna, Austria*

Received 4 June 2001; accepted in final form 14 August 2001

Berglund, Jessica J., Martin Riegler, Yevgeny Zolotarevsky, Etienne Wenzl, and Jerrold R. Turner. Regulation of human jejunal transmucosal resistance and MLC phosphorylation by Na^+-glucose cotransport. *Am J Physiol Gastrointest Liver Physiol* 281: G1487–G1493, 2001.—Na^+-nutrient cotransport-dependent regulation of paracellular permeability has been demonstrated in rodent intestine and human intestinal epithelial cell lines. In cell lines this regulation is associated with phosphorylation of myosin II regulatory light chain (MLC). However, the subcellular localization of phosphorylated MLC during this regulation has not been studied and regulation of paracellular permeability and MLC phosphorylation has not been studied in isolated human intestine. To evaluate these events in human jejunum, isolated mucosa was mounted in Ussing chambers, characterized electrophysiologically, and then immunostained using anti-phosphorylated MLC and anti-total MLC antisera. MLC phosphorylation was assessed by calculating the ratio of anti-phosphorylated MLC signal to anti-total MLC signal within defined regions. Transmucosal resistance of mucosae without active Na^+-glucose cotransport was 37 ± 3% greater than that of mucosae with active Na^+-glucose cotransport within 15 min. Quantitative double-label immunofluorescence showed that the phosphorylated MLC-to-total MLC ratio increased by 45 ± 4% within the perijunctional actomyosin ring when Na^+-glucose cotransport was active. Thus regulation of transmucosal resistance by Na^+-glucose cotransport is accompanied by increased MLC phosphorylation within the perijunctional actomyosin ring. These data support the proposed critical role of the perijunctional cytoskeleton in physiological regulation of human small intestinal paracellular permeability.

myosin II regulatory light chain; tight junction; perijunctional actomyosin ring; paracellular permeability; Na^+-glucose cotransporter

SMALL INTESTINAL MUCOSAL NUTRIENT absorption occurs primarily via active epithelial transport. In the case of glucose, active transport occurs at the apical, or luminal, surface of villus enterocytes via Na^+-glucose cotransporter (SGLT)1 (7, 15). Glucose then traverses the basolateral membrane through the facilitated glucose exchanger GLUT2. However, it has been suggested that paracellular glucose absorption serves to augment transcellular nutrient absorption (11, 17). Consistent with this hypothesis, paracellular absorption of inert tracers is increased in the presence of active Na^+-glucose cotransport (12, 18). This is also supported by mathematical modeling studies of the epithelial barrier in rat small intestine that demonstrates increased flux through small paracellular pores during active Na^+-glucose cotransport (4).

Use of a reductionist Caco-2 cell model has shown that Na^+-glucose cotransport-dependent regulation of paracellular permeability is associated with increased phosphorylation of the myosin II regulatory light chain (MLC), as detected in cell lysates (19). Such phosphorylation is a biochemical indicator of actomyosin contraction. On the basis of these data we hypothesized that the phosphorylated MLC might be localized to the perijunctional actomyosin ring, thereby allowing for physical interactions with the tight junction. To test this hypothesis we evaluated human jejunal mucosae that had been incubated under conditions of active or inactive Na^+-glucose cotransport by double-label quantitative immunofluorescence microscopy to assess perijunctional MLC phosphorylation. The data show that decreases in transmucosal resistance, a sensitive marker of increased paracellular permeability, occur after activation of Na^+-glucose cotransport and are accompanied by increased phosphorylation of perijunctional MLC in human jejunal absorptive (villus) enterocytes.

MATERIALS AND METHODS

Ussing chamber experiments. Surgically excised specimens of tumor-free jejunum isolated during pancreatoduodenectomy were used. Specimens were obtained from the first jejunal segment, immediately distal to the ligament of Treitz, and the seromuscular layer was removed by blunt dissection. Mucosal preparations (1.0-cm^2 surface area) from each specimen were vertically mounted in Ussing chambers (1.0-cm^2 surface area; Precision Instrument Design, Lake Tahoe, CA) as described previously (13). Luminal and serosal sides were bathed at 37°C in 8 ml of nutrient buffer containing (in mM) 122 NaCl, 2 $CaCl_2$, 1.3 $MgSO_4$, 5 KCl, 3 glucose, 22 mannitol, and 25 $NaHCO_3$ (pH 7.45 when gassed with 95% O_2-5% CO_2).

Address for reprint requests and other correspondence: J. R. Turner, Dept. of Pathology, Univ. of Chicago, 5841 South Maryland Ave., Mail Code 1089, Chicago, IL 60637 (E-mail: jturner@bsd.uchicago.edu).

The costs of publication of this article were defrayed in part by the payment of page charges. The article must therefore be hereby marked "*advertisement*" in accordance with 18 U.S.C. Section 1734 solely to indicate this fact.

Potential difference and short-circuit current (I_{sc}) were continuously measured and recorded every 1–10 min. Luminal and serosal solutions were connected via Ag-AgCl electrodes to a voltage/current clamp (model VCC600; Physiologic Instruments, San Diego, CA). Transmucosal resistance was calculated using Ohm's law from the open-circuit potential difference and the I_{sc}. Potential difference values were given in millivolts (lumen negative), I_{sc} values in microamperes per square centimeter, and transmucosal resistance in ohm-square centimeters. Potential difference and transmucosal resistance values were corrected for the junctional potentials (<0.1 mV) between luminal and serosal solutions and the buffer resistance, respectively, as described previously (13). The protocol for use of human tissues was approved by the Ethics Committee of the University Clinic of Vienna (Vienna, Austria).

After 20 min of equilibration, the mucosal buffer was exchanged for buffer with 25 mM glucose (and 0 mM mannitol) or 3 mM glucose, 22 mM mannitol, and 2 mM phloridzin. Phloridzin is a glucose analog that specifically inhibits SGLT1 but is not transported into cells and does not alter intracellular glucose metabolism. Previous studies have shown that 2 mM phloridzin is sufficient to inhibit SGLT1-mediated transport of 3 mM glucose and that this does not decrease intracellular ATP levels in cultured cell lines (19). Moreover, in isolated rodent tissue, phloridzin was able to prevent glucose-stimulated SGLT1-mediated regulation of transmucosal resistance without preventing a similar fall in transmucosal resistance triggered by Na^+-alanine cotransport (1), suggesting that phlorizdin is a specific inhibitor without relevant toxicities in these studies. Open-circuit potential difference and I_{sc} were measured for 30 min, after which the jejunal tissue was snap-frozen in optimal cutting temperature solution and stored at −80°C. Because regulation of transmucosal resistance by SGLT1-mediated Na^+-glucose cotransport is reversible (19), i.e., transmucosal resistance decreases when Na^+-glucose cotransport is activated and increases when Na^+-glucose cotransport is inhibited, the transmucosal resistance of mucosae with active Na^+-glucose cotransport was normalized to that of mucosae with inactive Na^+-glucose cotransport at each time point. Before normalization the data showed that, in addition to decreasing after activation of Na^+-glucose cotransport with 25 mM glucose, transmucosal resistance increased modestly after inhibition of Na^+-glucose cotransport with phloridzin, consistent with the demonstrated reversibility of this regulated process (19).

Anti-phosphorylated MLC antibody production. A phosphopeptide (R-P-Q-R-A-T-pS-N-V-F-A-C; pS = phosphoserine) corresponding to serine 19-phosphorylated MLC was commercially synthesized by Mimotopes (Raleigh, NC), and 5 mg of the phosphopeptide was conjugated to 31 mg of a carrier protein, diphtheria toxoid from the same company, as described previously (9). Two rabbits were immunized with 2.5% conjugated peptide emulsified in Freund's complete adjuvant, and immunization was boosted after 2 wk with the same antigen solution in Freund's incomplete adjuvant. Serum from both rabbits showed a strong reaction to MLC phosphorylated by MLC kinase but no reactivity with nonphosphorylated MLC (Fig. 1*A*). The antibody was affinity-purified with a column prepared using the SulfoLink kit (Pierce Chemical, Milwaukee, WI) and 2 mg of the unconjugated phosphopeptide. After elution from the affinity column fractions with the highest protein concentrations, as determined by absorbance at 280 nm, were dialyzed against PBS with 0.05% NaN_3.

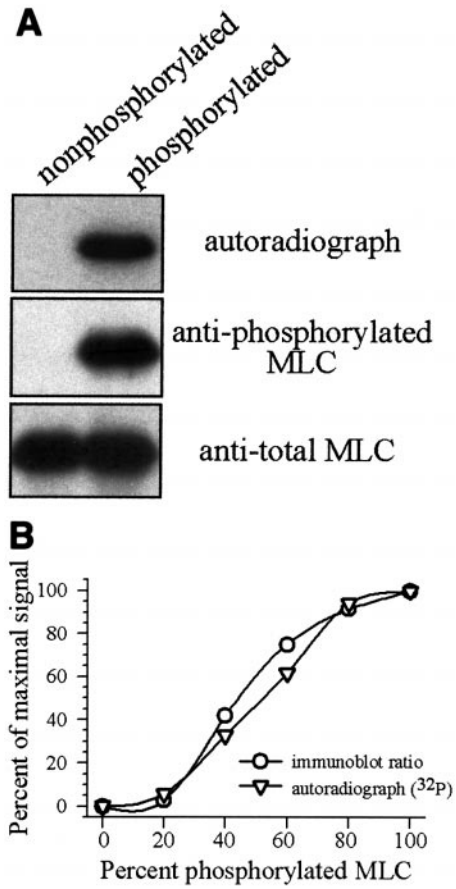

Fig. 1. Characterization of phosphospecific anti-myosin II regulatory light chain (MLC) antisera. *A*: rabbits were immunized with a phosphopeptide corresponding to residues 13–22 of serine 19-phosphorylated MLC. Antisera were affinity-purified using the same peptide. Purified recombinant human enterocyte MLC was (*right*) or was not (*left*) phosphorylated in vitro with purified MLC kinase and [^{32}P]ATP. These phosphorylated or nonphosphorylated MLC preparations were separated by SDS-PAGE and transferred to polyvinylidene difluoride. The autoradiograph (*top*) shows ^{32}P labeling only of phosphorylated MLC. *Middle*: immunoblot with the affinity-purified phosphospecific antisera showing that this antisera only reacts with phosphorylated MLC. *Bottom*: immunoblot with the polyclonal anti-total MLC antisera. This demonstrates equivalent reactivity of phosphorylated and nonphosphorylated MLC with the anti-total MLC antisera. *B*: samples of phosphorylated and nonphosphorylated MLC were mixed in varying proportions and separated by SDS-PAGE. Autoradiographs and immunoblots using the anti-phosphorylated MLC and anti-total MLC antisera were performed as in *A*, and the signal intensities were quantified. The autoradiograph values were normalized to the intensity of the sample that contained only phosphorylated MLC (▽), and the ratios of the immunoblot intensities using anti-phosphorylated MLC and anti-total MLC antisera were calculated and normalized to the ratio of the sample that contained only phosphorylated MLC (○). The curves generated by each data set were nearly identical (r = 0.96), thus confirming that the anti-phosphorylated MLC to anti-total MLC signal ratio reflects MLC phosphorylation quantitatively.

The quantitative binding of the anti-phosphorylated MLC antibody was compared with ^{32}P incorporation on Western immunoblots using preparations of recombinant human enterocyte MLC phosphorylated by Caco-2 intestinal epithelial cell myosin light chain kinase in the presence of [γ-^{32}P]ATP. A separate preparation containing an identical amount of MLC that was not phosphorylated was also prepared. The

phosphorylated and nonphosphorylated MLC preparations were mixed in varying proportions, keeping the total MLC constant. Total MLC was detected with a goat anti-MLC polyclonal antibody (Santa Cruz Biotechnology, Santa Cruz, CA) generated against an MLC-derived peptide distinct from the peptide used to generate the anti-phosphorylated MLC antibody. The immunoblot signal from the phosphorylated MLC immunoblot was normalized to the total MLC immunoblot signal of identical samples. Autoradiographs were performed using preflashed film. Immunoblot band intensities were determined using a Bio-Rad Fluor-S-Max and QuantityOne software (Bio-Rad, Hercules, CA). This analysis showed that the phosphorylated MLC-to-total MLC ratio was closely correlated with the ^{32}P autoradiograph signal (Fig. 1*B*; $r = 0.96$) and accurately reflected MLC phosphorylation.

Immunostaining. Frozen sections (3–5 μm) of the jejunal tissue were collected on coated slides and allowed to air dry at room temperature for 1 h. The sections were then fixed in 1% paraformaldehyde in PBS for 2 min. After three 5-min washes in PBS, nonspecific binding was blocked by a 15-min incubation in PBS with 5% (wt/vol) bovine serum albumin. Sections were incubated with affinity-purified anti-phosphorylated MLC and anti-total MLC (10 μg/ml each in PBS with 5% bovine serum albumin) overnight at room temperature in a humidified chamber. After four 5-min washes in PBS with 5% bovine serum albumin, sections were incubated for 1 h with Alexa 594-conjugated donkey anti-goat IgG (Molecular Probes, Eugene, OR) diluted in PBS with 5% bovine serum albumin. After four more washes in PBS with 5% bovine serum albumin, unoccupied binding sites for goat IgG were blocked by incubation for 30 min in PBS with 5% normal goat serum. Sections were then incubated with Alexa 488-conjugated goat anti-rabbit IgG (Molecular Probes) and 4′,6-diamidino-2-phenylindole (DAPI; 100 ng/ml) in PBS with 5% normal goat serum for 1 h at room temperature. After four washes in PBS with 5% normal goat serum, sections were washed once in PBS and rinsed once in water. They were then covered with 50 μl of Slowfade reagent in 50% glycerol (Molecular Probes), a coverslip was placed on top, and the coverslip was sealed with nail polish. After drying the slides were stored at −20°C. Samples stained for occludin and phosphorylated MLC were handled as above except that monoclonal anti-occludin (Zymed, South San Francisco, CA) and Alexa 594-conjugated goat anti-mouse IgG were substituted for the anti-total MLC detection regents.

Fluorescence microscopy. Sections were examined under a Leica DMLB epifluorescence microscope by an observer blinded to the experimental condition using a ×63 plan apochromatic oil immersion objective, A (DAPI), I3 (Alexa 488), and N2.1 (Alexa 594) filter cubes, and a SPOT RT monochrome digital camera (Diagnostic Instruments, Sterling Heights, MI). Control sections in which one or more fluorochromes were omitted during staining were used to confirm that the signal from each fluorochrome was only detectable with the specified filter settings. Images were collected using SPOT acquisition software version 3.0.4. Exposure was controlled manually and was identical for all images of each fluorochrome. For each field photographed, separate images were collected for each wavelength.

Image analysis. Image-Pro Plus 4.1 (Media Cybernetics, Silver Spring, MD) was used to analyze the collected images. Pseudocolor images were generated by adding color to each monochrome file to create an in-register color image showing one, two, or three fluorochromes. After creation of the color image files, entire multicolor image files were deconvolved using AutoDeblur (Autoquant Imaging, Watervliet, NY). Matched regions within individual deconvolved images showing different fluorochrome combinations were cropped and enlarged using Photoshop (Adobe Systems, San Jose, CA).

For quantitative analysis of MLC phosphorylation, identical areas of interest including the perijunctional actomyosin ring of villus enterocytes were selected (by an observer blinded to the experimental condition), based on pixel locations, in nondeconvolved monochrome anti-phosphorylated MLC and anti-total MLC images. Pixel-by-pixel intensity values were arranged by *x-y* coordinates and exported to MS Excel (Microsoft, Redmond, WA). Data for both anti-phosphorylated MLC and anti-total MLC images were individually filtered to include only higher-intensity pixels corresponding to the perijunctional actomyosin ring, based on a minimum intensity threshold, and to allow exclusion of aberrant bright spots. Alignment of the *x-y* coordinates was confirmed, and the ratios of anti-phosphorylated MLC and anti-total MLC intensities were calculated for each pixel pair. These values, typically representing the ratios of 3,000–4,000 pixels, were analyzed for mean and standard deviation, and outliers were sought (none were identified). The mean of the 1,500–2,000 ratios calculated from each pair of images was then considered a single measurement. A total of 213 such pixel-by-pixel analyses were performed, 105 from jejunal mucosae incubated without phloridzin and 108 from jejunal mucosae incubated with phloridzin. Statistical evaluation of the group ratio data was performed using Excel. Group comparisons were made with Student's *t*-test for unpaired samples.

RESULTS

SGLT1-mediated Na^+-glucose cotransport regulates transmucosal electrical resistance. To determine whether paracellular permeability is regulated by Na^+-glucose cotransport in human small intestinal mucosae, we measured transmucosal electrical resistance and I_{sc} in segments of human jejunum mounted in Ussing chambers. Initiation of Na^+-glucose cotransport led to the generation of an SGLT1-dependent I_{sc} of 26 ± 8 μA/cm^2, consistent with transmucosal Na^+ absorption. The transmucosal electrical resistance of mucosae with active Na^+-glucose cotransport was 85 ± 5%, 73 ± 3%, and 78 ± 6% of that of mucosae with inactive Na^+-glucose cotransport after 10, 15, and 30 min, respectively ($P < 0.01$ at each time point, $n = 5$; Fig. 2). Thus Na^+-glucose cotransport causes changes in transmucosal electrical resistance of human jejunum that are similar to those previously described in isolated rodent small intestinal mucosae and epithelial monolayers of human enterocyte cell lines (10, 19).

SGLT1-mediated Na^+-glucose cotransport is associated with increased phosphorylation of perijunctional MLC. Early studies of Na^+-glucose cotransport in rodent mucosae showed a striking condensation of the perijunctional cytoskeleton in association with increases in paracellular permeability (8). We have hypothesized that this is mediated by contraction of the perijunctional actomyosin ring that, in turn, is activated by phosphorylation of MLC, a biochemical indicator of actomyosin contraction (19). However, because previous studies have only evaluated MLC phosphorylation in lysates of cultured epithelial cell lines, it has not been possible to identify the subcellular location associated with increased MLC phosphorylation after initiation of Na^+-glucose cotransport. Thus, to evalu-

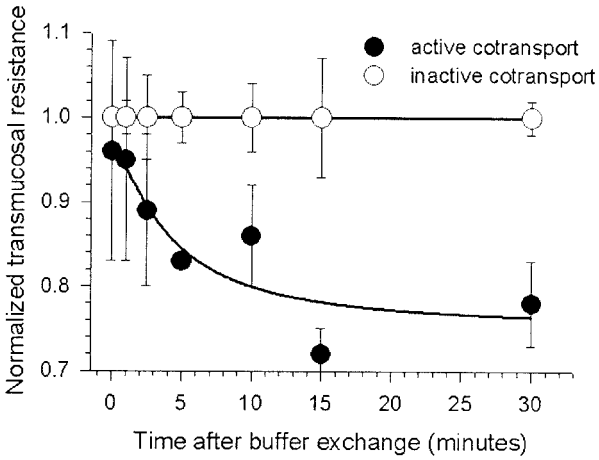

Fig. 2. Transmucosal resistance response to activation or inhibition of Na^+-glucose cotransport. Increasing the luminal glucose concentration to 25 mM caused decreases in transmucosal resistance after a lag of 10–15 min (●) relative to samples in which Na^+ glucose cotransport was inhibited (○). Data shown are means ± SE of duplicate samples from a single patient and are representative of 5 independent experiments with 5 different patients ($P < 0.01$ at time points after 5 min). Data at each time point are normalized to the transmucosal resistance of the samples with inactive Na^+-glucose cotransport.

ate MLC phosphorylation in intact mucosa and to determine the site of increased MLC phosphorylation, we evaluated perijunctional MLC phosphorylation in villus (absorptive) enterocytes from human jejunal mucosae that had been characterized electrophysiologically.

Our initial studies showed that the distribution of phosphorylated MLC was more restricted than that of total MLC, with the former being more greatly concentrated within the perijunctional actomyosin ring (Fig. 3). Moreover, the intensity of the phosphorylated MLC signal was increased at areas of cell-cell contact (Fig. 3). To determine whether these focal areas of increased phosphorylated MLC staining corresponded to the tight junction, we performed double-label immunofluorescence studies using the phosphospecific anti-MLC antibody and a monoclonal antibody against occludin, a transmembrane tight junction protein. Figure 4 shows that both phosphorylated MLC and occludin localize to areas of cell-cell contact. There is substantial overlap of the staining for phosphorylated MLC and occludin. Thus the cell junction-associated increases in phosphorylated MLC are partially localized within the tight junction, as defined by occludin distribution.

To quantify MLC phosphorylation we used a ratiometric double-label immunofluorescence approach. Preliminary studies demonstrated that the ratio of phosphorylated MLC signal (detected with the phosphospecific anti-MLC antibody; Fig. 1*A*) to total MLC signal was tightly correlated with MLC phosphorylation assessed by ^{32}P incorporation (Fig. 1*B*). Therefore, we employed this same approach to evaluate perijunctional MLC phosphorylation. The phosphorylated MLC-to-total MLC ratio was 1.60 ± 0.04 (range 3.13–1.02, $n = 105$; Fig. 5*A*) in villus enterocytes from jejunal mucosa with active Na^+-glucose cotransport. When villus enterocytes from jejunal mucosa with inactive Na^+-glucose cotransport were analyzed in an identical manner the phosphorylated MLC-to-total MLC ratio was 1.10 ± 0.03 (range 2.16–0.64, $n = 108$; Fig. 5*B*). This corresponds to a 45 ± 4% increase in the phosphorylated MLC-to-total MLC ratio when Na^+-glucose cotransport was active ($P < 0.001$; Fig. 6). Thus active Na^+-glucose cotransport is associated with increased phosphorylation of perijunctional MLC in human jejunal villus enterocytes.

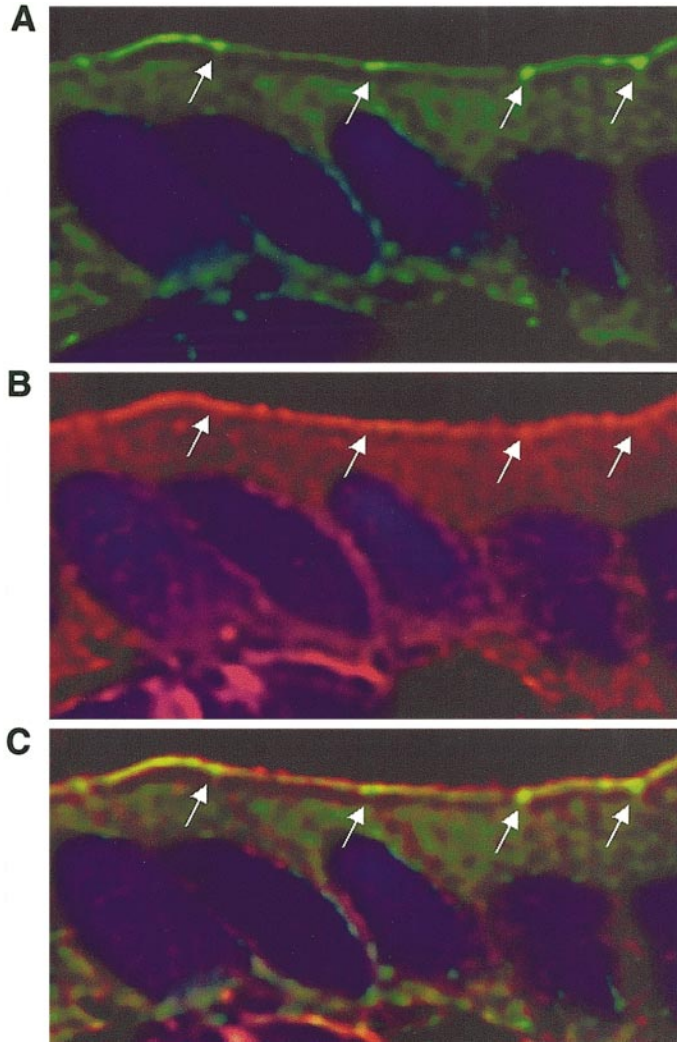

Fig. 3. Distributions of phosphorylated and total MLC in human jejunal mucosae. Human jejunal mucosae were doubly labeled by indirect immunofluorescence with the affinity-purified polyclonal anti-phosphorylated MLC antisera (green pseudocolor) and polyclonal anti-total MLC antisera (red pseudocolor). Nuclei were stained blue with DAPI (composite image, *C*). Control samples verified the absence of detectable green stain with the red filter set and vice versa. *A*: distribution of phosphorylated MLC in an area of villus mucosa. Focal intensification at areas of cell-cell junctions is noticeable (arrows). *B*: distribution of total MLC in the same field as *A*. *C*: composite image of *A* and *B* shows that the distribution of phosphorylated MLC is restricted to the perijunctional actomyosin ring, while that of total MLC is less constrained. Both phosphorylated MLC and total MLC are also detected in stromal cells beneath the basement membrane (*bottom left* of field).

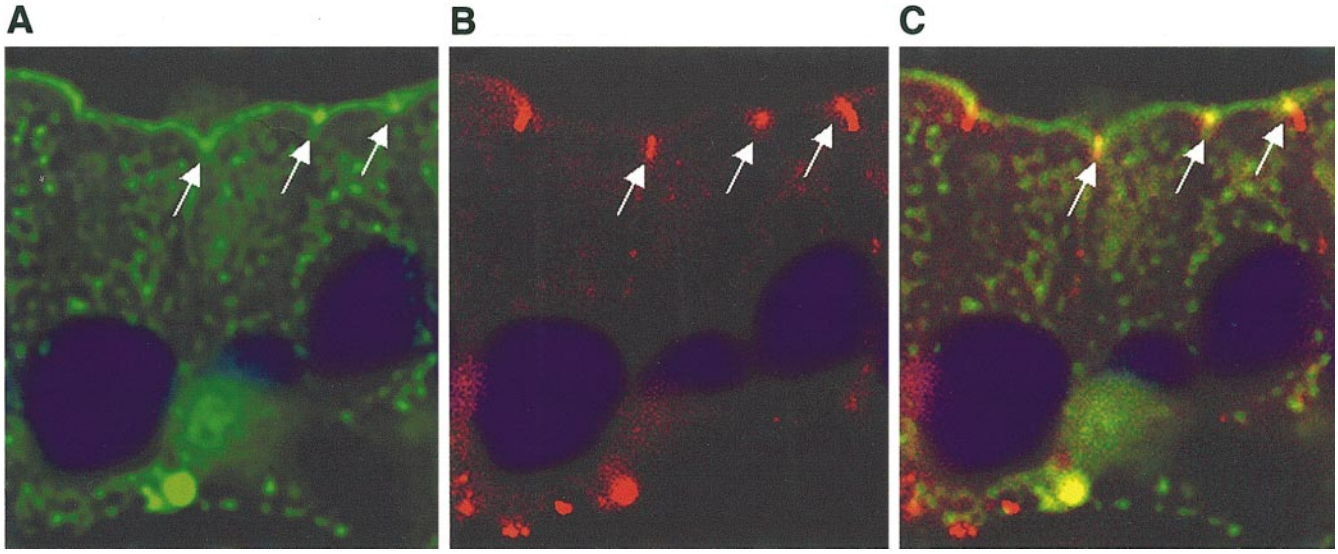

Fig. 4. Distributions of phosphorylated MLC and occludin in human jejunal mucosae. Human jejunal mucosae were double-labeled by indirect immunofluorescence with the affinity-purified polyclonal anti-phosphorylated MLC antisera (green pseudocolor) and monoclonal anti-occludin (red pseudocolor). Nuclei were stained with DAPI (blue pseudocolor). *A*: distribution of phosphorylated MLC in an area of villus mucosa, as seen in Fig. 3*A*, focal intensification at areas of cell-cell junctions is noticeable (arrows). This distribution is similar to that of the transmembrane tight junction protein occludin (red, *B*). There is significant, though incomplete, colocalization of phosphorylated MLC and occludin, as defined by the yellow areas in the composite photomicrograph (*C*).

DISCUSSION

Pappenheimer, Madara, and Reiss (8, 10, 12) demonstrated that Na^+-glucose cotransport caused a coordinated regulation of tight junction structure and paracellular permeability in rodent small intestine. This increase in paracellular permeability was also associated with increases in paracellular solute flux. On the basis of these observations, the authors proposed that paracellular absorption of small nutrients contributed to overall nutrient absorption. However, despite numerous studies, this hypothesis has remained controversial. For example, endoscopic studies of human subjects failed to identify any increase in paracellular solute flux during active Na^+-glucose cotransport (5, 6). Nevertheless, the in vitro observation that tight junction permeability is regulated by Na^+-glucose cotransport remains, and studies using transfected epithelial cell lines have shown that tight junction regulation after Na^+-glucose cotransport is associated with MLC phosphorylation (19). Although inhibitors of MLC kinase can prevent tight junction regulation in both transfected epithelial cell lines and isolated rodent mucosae (19), it has not been possible to document increases in enterocyte MLC phosphorylation in native mucosae. Moreover, because studies in cell lines have depended on cell lysates, the subcellular localization of phosphorylated MLC is unknown. Therefore, we sought to use established in vitro methods to evaluate the molecular basis of these events in intact mucosae. These studies of human jejunal mucosae show that regulation of transmucosal resistance by Na^+-glucose cotransport occurs in isolated human jejunal mucosae in a manner that is both qualitatively and quantitatively similar to that in isolated rodent mucosa and cultured epithelial monolayers (1, 19). Thus we concluded that human mucosa studied in this manner represented an acceptable model of Na^+-glucose cotransport-dependent regulation of transmucosal resistance.

Previous studies suggest that contraction of the perijunctional actomyosin ring, as indicated by MLC phosphorylation, is necessary for regulation of paracellular permeability in both cultured epithelial monolayers (19). However, the heterogeneity of cell types made such biochemical analyses impossible in native mucosae. We have used a phosphospecific anti-MLC antisera to evaluate MLC phosphorylation in isolated native human mucosae. This morphology-based approach allows us to limit our analysis to villus enterocytes only, without the potential for artifact introduced by other epithelial and nonepithelial cell types. Quantitative analysis demonstrated a 45 ± 4% increase in the phosphorylated MLC-to-total MLC ratio at the perijunctional actomyosin ring as a consequence of active Na^+-glucose cotransport. Moreover, these studies show that phosphorylated MLC is concentrated within the perijunctional actomyosin ring and is, therefore, physically linked to the tight junction, the primary determinant of paracellular permeability. Notably, the distribution of phosphorylated MLC was more restricted than that of total MLC and was enhanced in areas that, corresponded to the tight junction.

The molecular details responsible for the regulation of tight junction permeability via actomyosin contraction remain largely unknown, but the functional and structural association of the tight junction with the perijunctional actomyosin ring is well recognized (16). Moreover, a number of interactions between tight junc-

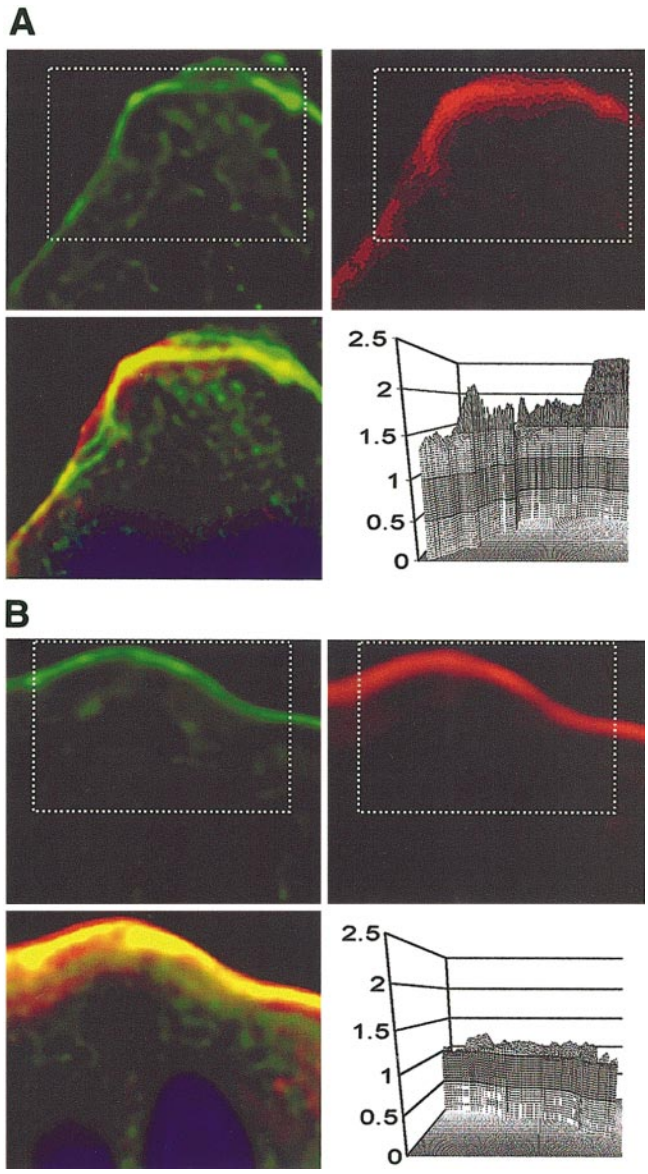

Fig. 5. Quantitative immunofluorescence of human jejunal mucosae. Specimens from Ussing chamber studies were double-labeled by indirect immunofluorescence as described in text. The specimens shown in this figure are representative samples from the mucosae studied electrophysiologically in Fig. 2. *A*: mucosae with active Na^+-glucose cotransport. A well-visualized area of villus enterocyte perijunctional MLC was imaged in the green pseudocolor channel (phosphorylated MLC) and the red pseudocolor channel (total MLC). The area of analysis is shown by the white boxes. Within this area a minimum threshold was applied to eliminate pixel intensity values from areas not within the bright perijunctional actomyosin ring. The images were precisely aligned, and the ratio of phosphorylated signal intensity to total MLC signal intensity was calculated on a pixel-by-pixel basis. The results for the 1,795 pixels included in this analysis are shown in the 3-dimensional graph with signal intensity on the vertical axis and pixel location on the horizontal axes. The mean for this analysis was 1.73. A total of 105 separate analyses were performed for mucosae with active Na^+-glucose cotransport. *B*: mucosae with inactive Na^+-glucose cotransport. The green pseudocolor channel (phosphorylated MLC) and red pseudocolor channel (total MLC) data within the area of analysis (white boxes) were analyzed as described for *A*. The mean for this analysis of 1,667 pixels was 1.08, which is representative of 108 separate analyses for mucosae with inactive Na^+-glucose cotransport.

tion proteins and actin have been described. In light of these biochemical data, ZO-1, a peripheral membrane protein localized to the cytoplasmic face of the tight junction (14), may be involved in the effects of MLC phosphorylation on tight junction permeability. ZO-1 is a member of the PDZ family of proteins that contain domains specialized to mediate for protein-protein interactions and has both actin binding and actin cross-linking properties (20). Other tight junction proteins, including ZO-2, ZO-3, and occludin, also bind to actin (20), and the tight junction protein cingulin interacts with ZO-1, ZO-2, and ZO-3, as well as enterocyte myosin heavy chain (3). On the basis of these in vitro data, numerous functional interactions between the tight junction and perijunctional actomyosin ring are possible. However, at present, analysis of these interactions within epithelial cells is lacking.

Previous analyses of rodent mucosae have shown that capacitance and conductance are both increased by Na^+-glucose cotransport, indicative of increases in membrane surface area and width of intercellular junctions, respectively (10). This is consistent with contraction of the perijunctional actomyosin ring, as would be triggered by MLC phosphorylation. However, we were unable to detect decreases in the dimensions of the perijunctional actomyosin ring. We were also unable to detect any changes in inter-tight junction dimensions (as delineated by immunostaining with antibodies to the tight junction proteins occludin and ZO-1; unpublished observations). Nevertheless, the lack of gross changes in these dimensions is not surprising, because previous ultrastructural studies were also unable to detect changes in these cell dimensions (2, 8).

In summary, these studies show for the first time that the paracellular permeability of human jejunum, as demonstrated by transmucosal resistance, is regulated by Na^+-glucose cotransport. This regulation is associated with increases in MLC phosphorylation within villus absorptive enterocytes. The localization of

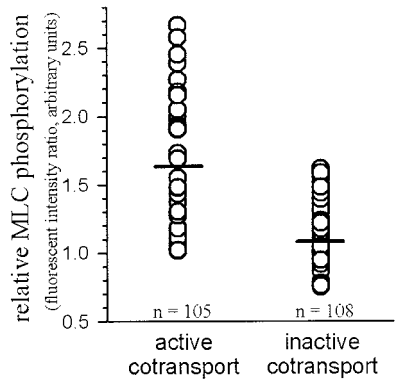

Fig. 6. Relative changes in perijunctional MLC phosphorylation in human jejunal mucosae with active or inactive Na^+-glucose cotransport. The relative phosphorylated MLC content of the perijunctional region of mucosae with active or inactive Na^+-glucose cotransport was determined for a total of 213 specimens as described in text. The mean phosphorylated MLC-to-total MLC ratios were 1.60 ± 0.04 and 1.10 ± 0.03, respectively, corresponding to an increase in phosphorylated MLC content of $45\% \pm 4$ ($P < 0.001$).

these increases in perijunctional MLC to the perijunctional actomyosin ring, with enhanced MLC phosphorylation at the apical junctional complex, supports a model of cytoskeletally mediated tight junction regulation.

We are grateful to Drs. Yasuharu Sasaki, Katsuhiko Sakurada, and Fumio Matsumura for sharing the anti-phosphorylated MLC antibodies that were used in our preliminary studies.

This work was supported by National Institute of Diabetes and Digestive and Kidney Diseases Grants DK-02503 and DK-56121.

REFERENCES

1. **Atisook K, Carlson S, and Madara JL.** Effects of phlorizin and sodium on glucose-elicited alterations of cell junctions in intestinal epithelia. *Am J Physiol Cell Physiol* 258: C77–C85, 1990.
2. **Atisook K and Madara JL.** An oligopeptide permeates intestinal tight junctions at glucose-elicited dilatations. Implications for oligopeptide absorption. *Gastroenterology* 100: 719–724, 1991.
3. **Cordenonsi M, D'Atri F, Hammar E, Parry DA, Kendrick-Jones J, Shore D, and Citi S.** Cingulin contains globular and coiled-coil domains and interacts with ZO-1, ZO-2, ZO-3, and myosin. *J Cell Biol* 147: 1569–1582, 1999.
4. **Fihn BM, Sjoqvist A, and Jodal M.** Permeability of the rat small intestinal epithelium along the villus-crypt axis: effects of glucose transport. *Gastroenterology* 119: 1029–1036, 2000.
5. **Fine KD, Santa Ana CA, Porter JL, and Fordtran JS.** Effect of D-glucose on intestinal permeability and its passive absorption in human small intestine in vivo. *Gastroenterology* 105: 1117–1125, 1993.
6. **Fine KD, Santa Ana CA, Porter JL, and Fordtran JS.** Mechanism by which glucose stimulates the passive absorption of small solutes by the human jejunum in vivo. *Gastroenterology* 107: 389–395, 1994.
7. **Hediger MA, Coady MJ, Ikeda TS, and Wright EM.** Expression cloning and cDNA sequencing of the Na^+/glucose cotransporter. *Nature* 330: 379–381, 1987.
8. **Madara JL and Pappenheimer JR.** Structural basis for physiological regulation of paracellular pathways in intestinal epithelia. *J Membr Biol* 100: 149–164, 1987.
9. **Matsumura F, Ono S, Yamakita Y, Totsukawa G, and Yamashiro S.** Specific localization of serine 19 phosphorylated myosin II during cell locomotion and mitosis of cultured cells. *J Cell Biol* 140: 119–129, 1998.
10. **Pappenheimer JR.** Physiological regulation of transepithelial impedance in the intestinal mucosa of rats and hamsters. *J Membr Biol* 100: 137–148, 1987.
11. **Pappenheimer JR.** On the coupling of membrane digestion with intestinal absorption of sugars and amino acids. *Am J Physiol Gastrointest Liver Physiol* 265: G409–G417, 1993.
12. **Pappenheimer JR and Reiss KZ.** Contribution of solvent drag through intercellular junctions to absorption of nutrients by the small intestine of the rat. *J Membr Biol* 100: 123–136, 1987.
13. **Riegler M, Sedivy R, Pothoulakis C, Hamilton G, Zacherl J, Bischof G, Cosentini E, Feil W, Schiessel R, LaMont JT, and Wenzl E.** *Clostridium difficile* toxin B is more potent than toxin A in damaging human colonic epithelium in vitro. *J Clin Invest* 95: 2004–2011, 1995.
14. **Stevenson BR, Siliciano JD, Mooseker MS, and Goodenough DA.** Identification of ZO-1: a high molecular weight polypeptide associated with the tight junction (zonula occludens) in a variety of epithelia. *J Cell Biol* 103: 755–766, 1986.
15. **Turk E, Zabel B, Mundlos S, Dyer J, and Wright EM.** Glucose/galactose malabsorption caused by a defect in the Na+/glucose cotransporter. *Nature* 350: 354–356, 1991.
16. **Turner JR.** "Putting the squeeze" on the tight junction: understanding cytoskeletal regulation. *Semin Cell Dev Biol* 11: 301–308, 2000.
17. **Turner JR.** Show me the pathway! Regulation of paracellular permeability by Na^+-glucose cotransport. *Adv Drug Delivery Rev* 41: 265–281, 2000.
18. **Turner JR, Cohen DE, Mrsny RJ, and Madara JL.** Noninvasive in vivo analysis of human small intestinal paracellular absorption: regulation by Na^+-glucose cotransport. *Dig Dis Sci* 45: 2122–2126, 2000.
19. **Turner JR, Rill BK, Carlson SL, Carnes D, Kerner R, Mrsny RJ, and Madara JL.** Physiological regulation of epithelial tight junctions is associated with myosin light-chain phosphorylation. *Am J Physiol Cell Physiol* 273: C1378–C1385, 1997.
20. **Wittchen ES, Haskins J, and Stevenson BR.** Protein interactions at the tight junction. Actin has multiple binding partners, and ZO-1 forms independent complexes with ZO-2 and ZO-3. *J Biol Chem* 274: 35179–35185, 1999.